Progress In Electromagnetics Research M, Vol. 119, 177–188, 2023

Mutual Coupling Reduction in UWB-MIMO Antenna Using Circular Slot EBG Structures

Raveendrababu Pakala[1, *] and Ramakrishna Dasari[2]

Abstract—In this paper, a compact Ultra Wide Band (UWB) Multiple Input Multiple Output (MIMO) antenna using circular slots Electromagnetic Band Gap (EBG) structures operating in frequency band from 3.1 GHz to 10.6 GHz is presented. The size of this compact antenna is $26 \times 33\,\text{mm}^2$. In wireless communications, such as WLAN, 4G, and 5G, MIMO has become an essential element. However, the major limiting factor of MIMO systems is mutual coupling due to the smaller spacing between multiple antennas, which reduces spatial diversity, antenna gain and can also result in unwanted interference and cross-talk between antenna elements. To enhance antenna performance and reduce the mutual coupling, EBG structures are used. Incorporation of EBG structures in MIMO antenna eliminates surface wave propagation, which reduces the mutual coupling. In this work, the design of a dot notch shaped UWB-MIMO antenna with a circular slot EBG structure is proposed. Results presented here are simulated by using CST microwave software studio. From the results it can be observed that the proposed antenna has bandwidth of 3.1 GHz–10.6 GHz. It exhibits 6.72 dB peak gain and reduces the mutual coupling considerably, i.e., more than −28 dB.

1. INTRODUCTION

Microstrip antenna is a widely used antenna due to its attractive features such as being compact in size, cost effective, planar structure, easy in fabrication, suitable to use in integrated circuits and compact devices. Easy feed of microstrip antenna makes it suitable for array antenna and Multiple-Input Multiple-Output (MIMO) systems [1]. The rapid growth in wireless communication technologies has the capability to connect many devices where MIMO system plays an important role. To connect all such devices, a wide spectrum is required. However, the available spectrum is limited. An alternative way to utilize the available spectrum effectively is MIMO communication. MIMO system has the capability to fulfil the demands such as increased channel capacity and high data rates with high quality and reliability for various applications. A suitable technology is provided by MIMO systems to accomplish these requirements without the requirement of extra bandwidth [2–4]. However, in most of the applications, a compact antenna is required where antenna dimensions and mutual coupling are the major challenge for MIMO designers. In general, decoupling within MIMO antennas involves the process of mitigating or eliminating the mutual coupling that occurs between individual antenna elements within a MIMO antenna array. Mutual coupling arises when the electromagnetic fields generated by one antenna element interfere with neighboring elements, resulting in signal interference and a degradation in the MIMO system's performance. Decoupling is a critical concept in MIMO systems as it is essential for preserving the independence of antenna elements, the prerequisite for realizing the full potential of MIMO technology. The key aspects of decoupling in MIMO antennas are Interference Mitigation, Enhanced Channel Independence, Physical Separation, Utilizing

Received 5 August 2023, Accepted 30 September 2023, Scheduled 8 October 2023
* Corresponding author: Raveendrababu Pakala (praveendrababu@cmrcet.ac.in).
[1] CMR College of Engineering Technology, Hyderabad, University College of Engineering, Osmania University, Hyderabad, India.
[2] University College of Engineering, Osmania University, Hyderabad, India.

Isolation Structures, Optimizing Antenna Design, Balancing Impedance, and Frequency Selectivity. Various decoupling techniques are available to reduce mutual coupling such as decoupling networks, neutralization lines, ground plane modifications, frequency-selective surface (FSS) or meta surface walls and electromagnetic band gap (EBG) structures. The best solution to reduce the isolation in MIMO is EBG structures, which helps to minimize the mutual coupling between antennas. The advantage of EBG structures is that the energy radiated in opposite direction is minimized which minimizes the surface current on the common ground [5–8]. Various techniques [9–14] have been proposed for the reduction of mutual coupling. Furthermore, for improving the isolation in MIMO systems, several methods have been established [15–23]. These methods include a coplanar waveguide-fed UWB-MIMO antenna that exhibits the isolation of -20 dB, and ECC is about 0.007 [15]. UWB of frequency band 3.1 and 13.5 GHz, in which the isolation of -23 dB and ECC less than 0.09 are achieved by using a modified electromagnetic band gap (MEBG) structure [16]. A compact modified hexagonal-shaped circular MIMO antenna is presented where its operating frequency band is from 2.95 to 6.3 GHz [17]. By using two radiating patches (a semicircle and a semi-regular hexagon), the performance (return loss and isolation) of multiband two-port MIMO antenna is demonstrated and it covers the frequency bands of 0.67–7.29 GHz, 8.07–12.11 GHz, 14.07–15.41 GHz, and 16.04–22 GHz in [18]. A MIMO antenna array structure which consists of 8 circular and semi-circular slots is presented in [19]. The array of rectangle-shaped slotted patch antennas with defected rectangular, circular, and a zigzag-shaped slotted structure is discussed in [20]. A simple geometry of a parasitic element to improve the isolation [21] and an isolation of (> -23 dB) are achieved by employing spatial and polarization diversity techniques [22]. [23–25] propose the reduction of mutual coupling by using a ladder resonator. Defected Ground Structures (DGSs) [26, 27] are preferred for enhancing the bandwidth of a compact, uni-planer UWB-MIMO antenna [28]. In [29] to improve the isolation, both ground stub and single column EBG structure were embedded in a MIMO antenna. A protruded ground branch structure in a compact owl-shaped MIMO antenna was implemented [30], and a shared radiator MIMO antenna was presented [31] for broad band application. In all these approaches, the structures of the antennas are complex, large in size, and isolation is not achieved in the entire UWB. In this work, to achieve the improved isolation in full UWB range, a compact UWB-MIMO antenna is designed by using a circular slots Electromagnetic Band Gap (EBG), which exhibits an isolation of more than -28 dB in the entire UWB frequency from 3.1 GHz to 10.6 GHz.

2. ANTENNA DESIGN

In this article, the transformation of UWB-MIMO antenna with EBG structures was explained in four phases i.e., Dot notch shaped MIMO antenna with Defective Ground Structure (Design-1), Dot notch shaped MIMO antenna with a Defective Ground Structure ground stub (Design-2), MIMO antenna with Defective Ground Structure, ground stub & Circular slot EBGs (Design-3), and finally, the design with Dot notch shaped antennas with Defective Ground Structure, ground stub & circular slot EBGs in T model (Final design). The details are explained in subsequent sections.

2.1. Dot Notch Shaped MIMO Antenna with Defective Ground Structure

The basic MIMO antenna of two identical dot notch rectangular patch antenna elements is printed on an FR-4 substrate with a dielectric constant of 4.3. The dimensions are measured as $26 \times 31\,\text{mm}^2$, and thickness is 0.8 mm, and a DGS is also incorporated in the design named as design-1 as shown in Figures 1(a) and 1(b). For both patch antennas, an inset feed-line is employed to match the 50 ohm characteristic impedance line. The top layer of FR-4 is used to create the feed line for two rectangular antennas, while the bottom layer is used as ground plane. The major challenging task is to fit the optimum EBG structure between the two antenna elements. In order to achieve both (i.e., compact size and minimal mutual coupling), 8 mm spacing is recommended for the proposed MIMO antenna. To increase the isolation between MIMO antenna elements, the distance between the antenna elements must be increased. Since one of the goals of this work is to develop a compact MIMO antenna, spacing between the components cannot be increased. The dimensions of this design are shown in Table 1. The simulated results achieved in this design are shown in Figures 2 to 7, and the bandwidth achieved in

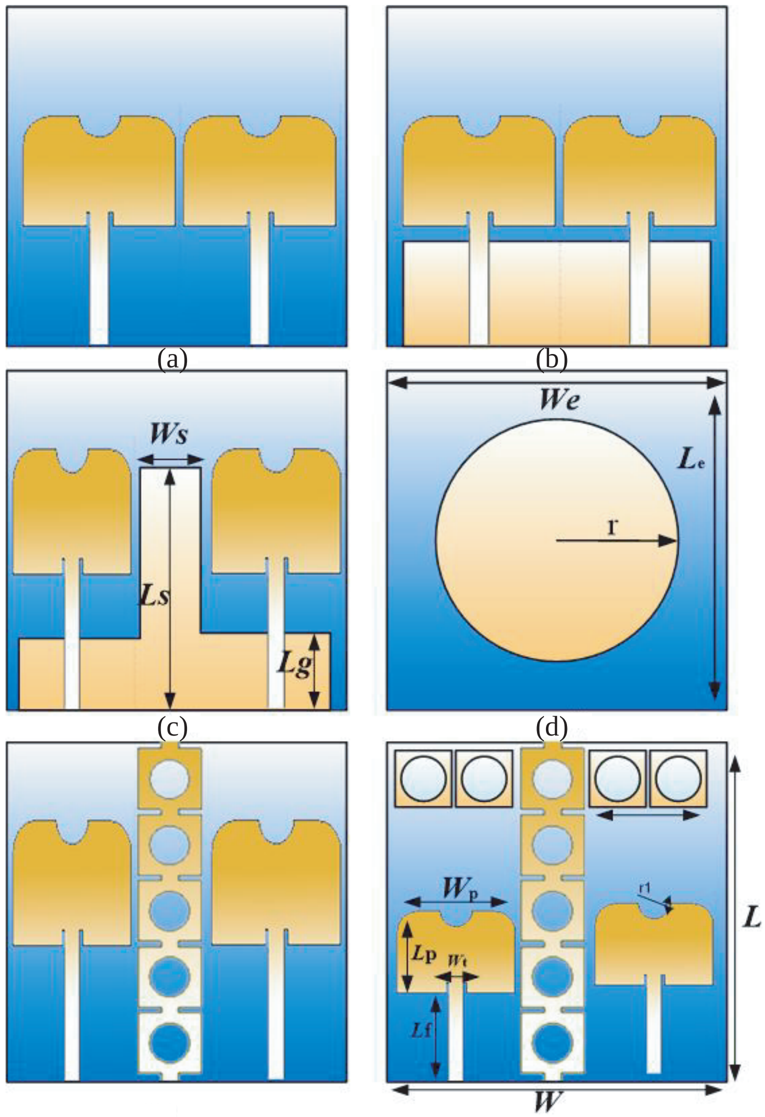

Figure 1. The evolution of proposed antenna design, (a) MIMO antenna, (b) MIMO antenna with defected ground structure, (c) MIMO antenna with ground stub, (d) unit cell of circular shaped EBG, (e) MIMO antenna with circular slot EBG structure, (f) MIMO antenna with circular slot EBGs in Tshape structure.

this design is between 5 and 9 GHz, which is not full UWB range. The isolation between antennas is nearly -10 dB, gain 2.5 dB, and group delay 3 ns. In this case, the UWB range is not achieved, and gain is also less. To improve the bandwidth for UWB range, the ground stub was added into the design.

The lower resonance frequency (fr) of the rectangular microstrip patch antennas can be given by:

$$fr = \frac{144}{lg + l1 + gp + \dfrac{w}{2\pi\sqrt{1+\epsilon r}} + \dfrac{w1}{2\pi\sqrt{1+\epsilon r}}}\ \text{GHz} \tag{1}$$

The planar microstrip antenna is designed according to Eq. (1), where "lg" is the length of the ground plane, "$l1$" used for the length of the patch element, and "gp" for the distance between the ground plane and the patch element. The widths of the substrate and patch element are denoted by letters "w" and "$w1$", respectively. Utilising the specified values given in Table 1, the lower resonance

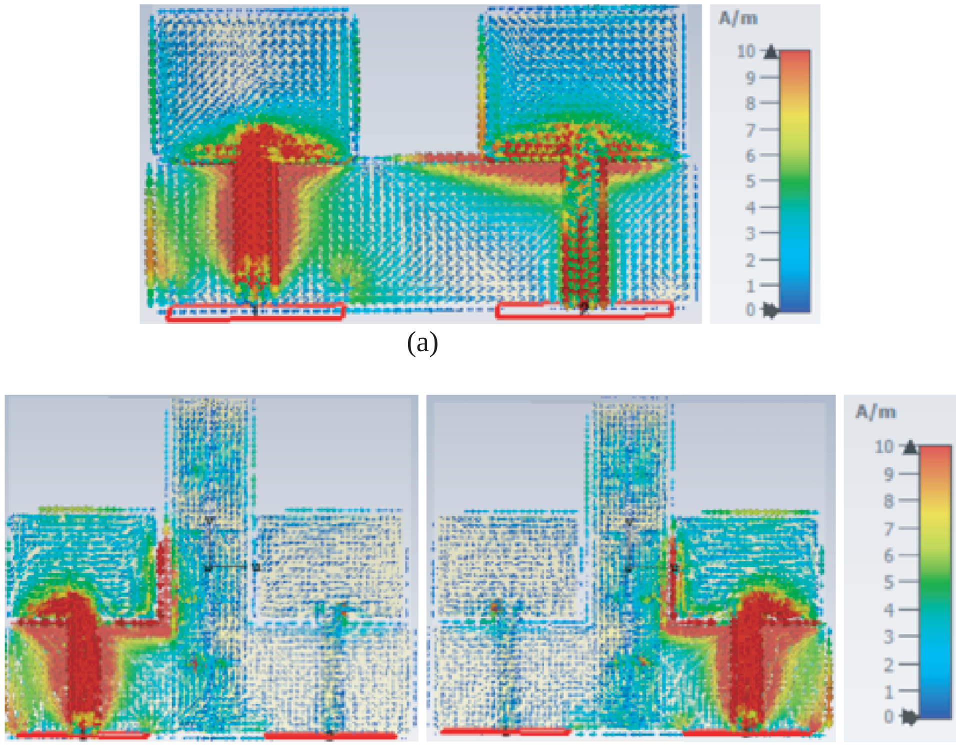

(a)

(b)

Figure 2. Comparison of current distribution, (a) without EBG, (b) with EBG.

frequency is 7.25 GHz, which is consistent with the resonance frequency of microstrip antenna. The stages of the design evolution are shown in Figures 1(a) to 1(f).

2.2. Dot Notch Shaped MIMO Antenna with DGS and Ground Stub

In order to minimize the mutual coupling between the two rectangular patches and to achieve UWB band range, i.e., 3.1 GHz to 10.6 GHz, a ground stub of width 'WS' and length 'LS' is embedded and named as design-2 as shown in Figure 1(c). The dimensions are mentioned in Table 1. The simulated results achieved in this design are shown in Figures 3 to 7. With this design, the bandwidth is improved to 3.1–10.6 GHz, isolation < -25 dB, gain 5.56 dB, and group delay 2 ns.

Table 1. Antenna parameters.

Parameters	Dimensions (mm)	Parameters	Dimensions (mm)
Length of substrate-FR4 (L)	26	Width of feedline (W_f)	1.4
Width of substrate-FR4 (W)	31	Thickness of patch and ground (t)	0.035
Height of substrate (h)	0.8	Length of ground stub (L_S)	26
Length of ground (L_g)	8.2	Width of ground stub (W_s)	6
Length of patch (L_p)	8	Length of the EBG (L_e)	4.6
Width of patch (W_p)	11	Width of the EBG (W_e)	4.8
Length of feedline (L_f)	10	Radius of circular slot (r)	1.5

2.3. Dot Notch Shaped MIMO Antenna with DGS, Ground Stub and Circular Slot EBGs

Further, to improve the gain of the proposed antenna and isolation (mutual coupling reduction), the EBG structure is added between two antennas into the design. The unit cell of circular slot EBG with radius 'r' and one dimensional circular slot EBG between antennas are shown in Figures 1(d) and 1(e) named as design-3, and dimensions are shown in Table 1. There was an improvement in the antenna performance such as isolation < -26 dB, gain about 5.83 dB, and group delay less than 2 ns. The simulated results achieved in this design are shown in Figures 3 to 7.

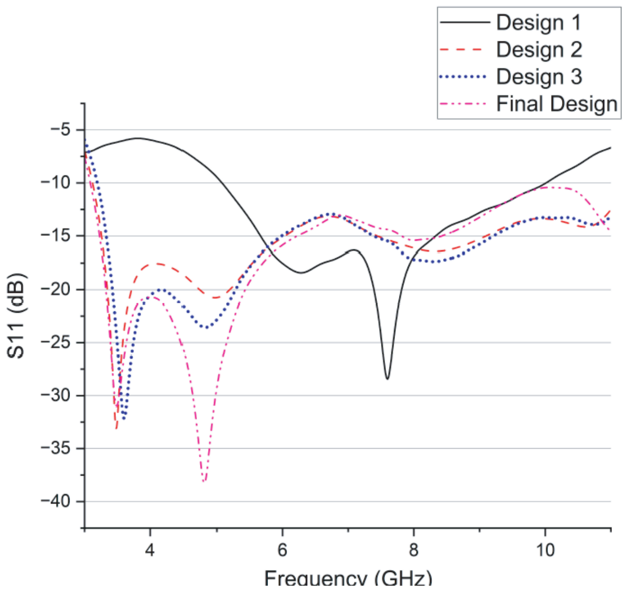

Figure 3. Comparison of various simulated results (S_{11}).

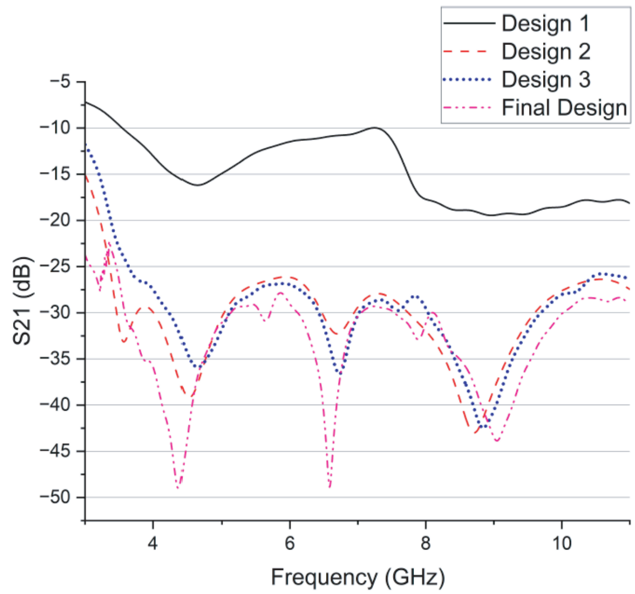

Figure 4. Comparison of various simulated results (S_{21}).

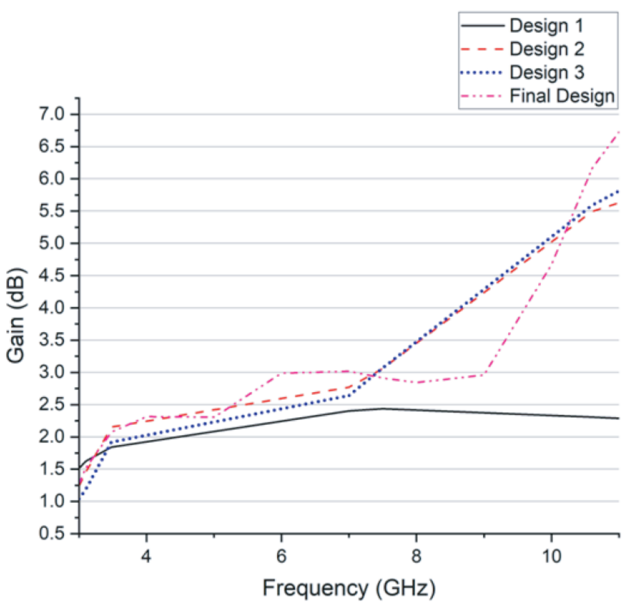

Figure 5. Comparison of various simulated results (GAIN).

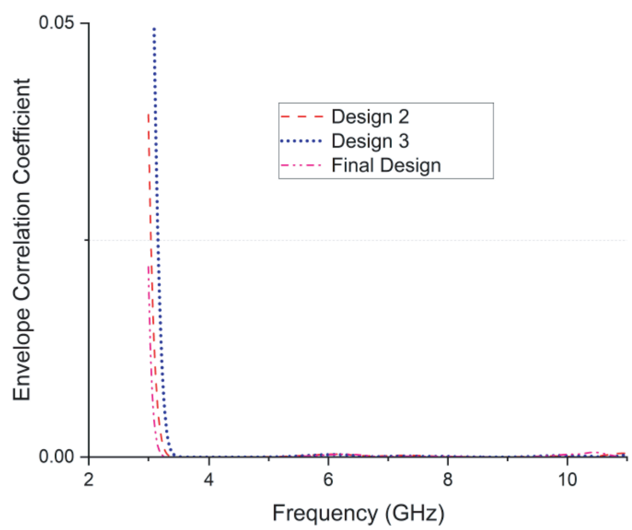

Figure 6. Comparison of various simulated results (ECC).

2.4. Dot Notch Shaped MIMO Antenna with DGS, Ground Stub and Circular Slot EBGs of T-Shaped Structure

Further, to reduce the mutual coupling between MIMO antennas and to improve the gain of proposed antenna, an extra circular slots EBG structure is added with T-shape model shown in Figure 1(f). With this proposed structure, more than < -28 dB of isolation is achieved in entire UWB; peak gain also increases about 6.72 dB; and group delay is less than 2 ns. The simulated results achieved in this design are shown in Figures 2 to 7.

3. RESULTS AND DISCUSSION

The various antenna parameters such as return loss (S_{11}), isolation S_{21}/S_{12}, gain, Envelope Correlation Co-efficient (ECC), group delay, and diversity gain of the proposed antenna were measured in the different stages of antenna transformation. The comparison is shown in Table 2. A few antenna parameters which are going to be calculated are discussed as follows:

Envelop Correlation Coefficient

In MIMO antennas for the assessment of diversity performance, Envelop Co-relation Coefficient (ECC) is one of the important parameters. Two methods are used to calculate ECC. One is based on the far-field pattern, which involves complex calculations and time consuming. The other method which is comparatively easy is from the scattering parameters of the antenna. Therefore, for the proposed antenna, the second method is adopted for calculating the ECC [20].

$$ECC = \frac{|S_{11}^* S_{12}^* + S_{21}^* S_{22}^*|^2}{(1 - |S_{11}|^2 - |S_{21}|^2|)(|1 - |S_{22}|^2 - |S_{12}|^2)} \tag{2}$$

Ideally, for uncorrelated antennas ECC should be zero. However, in MIMO antenna the acceptable value is less than 0.5. The ECC did not follow UWB in Design 1, but after adding ground stub, the MIMO antenna operates at UWB frequency and shows that ECC < 0.01, and after adding EBG structures, ECC value is further reduced.

Diversity Gain

Another significant parameter in the design of MIMO antenna is diversity gain (DG). It can be given by the formula:

$$DG = 10 * \sqrt{1 - ECC^2} \tag{3}$$

For satisfactory operation, the DG value should be close to 10 dB in a MIMO antenna [21]. In proposed work, the calculated value of DG is listed in Table 3, and it is greater than 9.995 for the entire operating frequency band.

3.1. Simulation Results of Antenna

The simulated results of proposed antenna in various stages are shown in Figures 2 to 7, and comparison of the antenna parameters in various stages of antenna design transformation is tabulated in Table 2. Figure 2 represents the current distribution in the antenna without and with an EBG structure. Figure 3 represents the return loss (S_{11}) comparison of proposed antenna in various stages from design -1 to final design as: design-1 representing the MIMO antenna with DGS shows reflection coefficient approximately -10 dB from 5 GHz to 9 Hz; design-2 with an added ground stub shows greater change in S_{11}, i.e., < -10 dB from 3.1 GHz to 10.6 GHz (UWB frequency); deigns 3, 4 with circular slot EBG structures show significant reduction in the return loss and achieve peak return loss around -40 dB.

Figure 4 represents the simulation results of transmission coefficient (mutual coupling between antennas), i.e., S_{21} for all the designs, i.e., from deign-1 to design-4. It can be observed that design-1, which represents the MIMO antenna with DGS, shows > -10 dB from 5 GHz to 9 Hz; design-2 with an added ground stub shows greater change in S_{21}, i.e., > -25 dB from 3.1 GHz to 10.6 GHz (UWB frequency); deigns-3 with circular slot EBG structures shows > -26 dB; and for design-4, i.e., final design, the return loss is greater than -28 dB in the entire UWB range.

Table 2. Comparison of various antenna designs.

Design	**S_{11} (dB)**	**S_{21} (dB)**	**Peak Gain (dB)**	**ECC**	**Group Delay (ns)**	**Diversity Gain**
Dot notch shaped MIMO antenna with Defective Ground Structure (Design-1)	< -10 dB (5 GHz–9 GHz)	< -10 dB (5 GHz–9 GHz)	2.5	< 0.01 (5 GHz–9 GHz)	< 3 ns	> 9.99
Dot notch shaped Ground Structure and ground stub (Design-2)	< -10 dB (3.1 GHz–10.6 GHz)	< -25 dB (3.1 GHz–10.6 GHz)	5.56	< 0.01 (3.1 GHz–10.6 GHz)	< 2 ns	> 9.99
MIMO Antenna with Ground structure, ground stub and Circular slot EBGs (Design-3)	< -10 dB (3.1 GHz–10.6 GHz)	< -26 dB (3.1 GHz–10.6 GHz)	5.83	< 0.01 (3.1 GHz–10.6 GHz)	< 2 ns	> 9.99
Dot Notch Shaped Antenna with circular slot EBGs in T mode (Final Design)	< -10 dB (3.1 GHz–10.6 GHz)	< -28 dB (3.1 GHz–10.6 GHz)	6.72	< 0.01 (3.1 GHz–10.6 GHz)	< 2 ns	> 9.99

Antenna gain is one of the most important parameters which is also improved by adding EBG structures in the horizontal row. Initially, the gain was about 2.45 dB with DGS, and it was improved to 5.6 dB by adding a ground stub. By introducing EBG structures, maximum peak gain of 6.72 dB is achieved as shown in Figure 5.

The Envelope Correlation Co-efficient (ECC) did not follow UWB in design 1, but after adding ground stub, the MIMO antenna operates at UWB frequency and shows ECC < 0.01. Adding EBG structures further more reduces the value of ECC as shown in Figure 6. The group delay for all the designs is less than 2 ns as shown in Figure 7. The diversity gain is about 9.99 for all the designs.

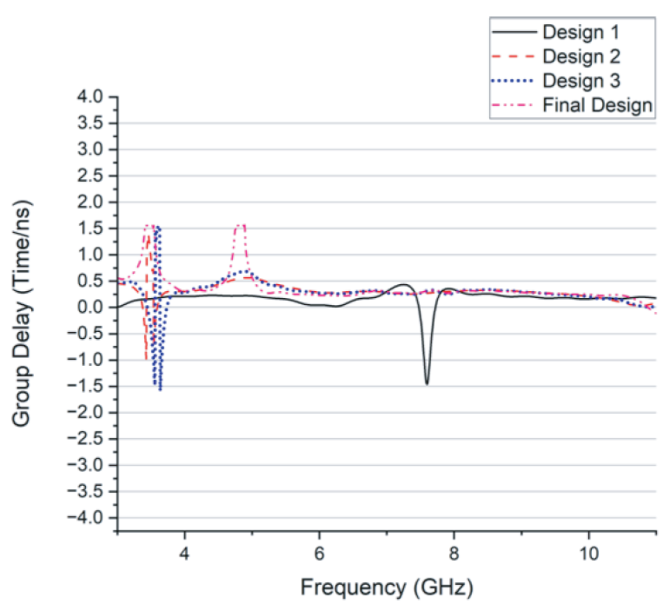

Figure 7. Comparison of various simulated results (GROUP DELAY).

3.2. Fabricated Antenna

On the basis of the above design procedure, a MIMO antenna is fabricated on a low-cost FR-4. Figure 8 shows fabricated antenna with circular slot EBG structures. Results depicted in Figures 9, 10, and 12 show the comparison of simulated antenna and fabricated antenna results.

Figure 8(a) shows the fabricated antenna front view with circular slots EBG structure, and Figure 8(b) represents the back view of proposed antenna. The size of the fabricated antenna is $26 \times 31\,\text{mm}^2$ with a Dot Notch shape of the patch.

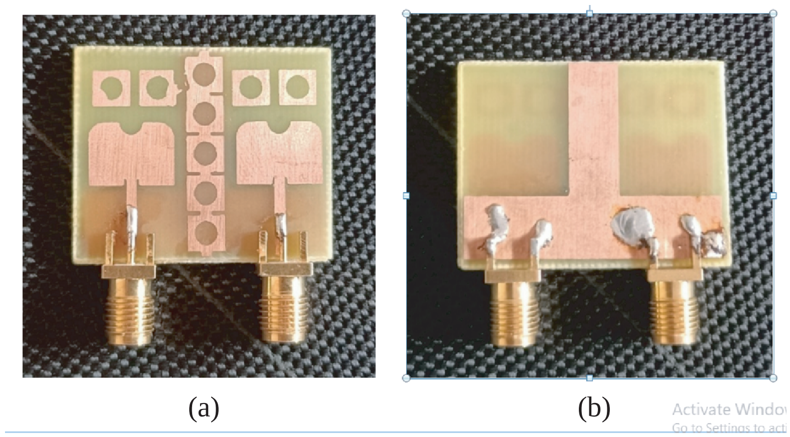

Figure 8. Physical antenna, (a) fabricated front view, (b) fabricated back view.

The comparison graph of simulated and measured results is drawn using ORIGIN PRO. It can be observed from Figures 9, 10, and 12 that the variation in simulated and fabricated antenna results are within the accepted level. It is observed that S_{11}, S_{21}, and radiation pattern of the fabricated antenna are in-line with the simulated antenna results.

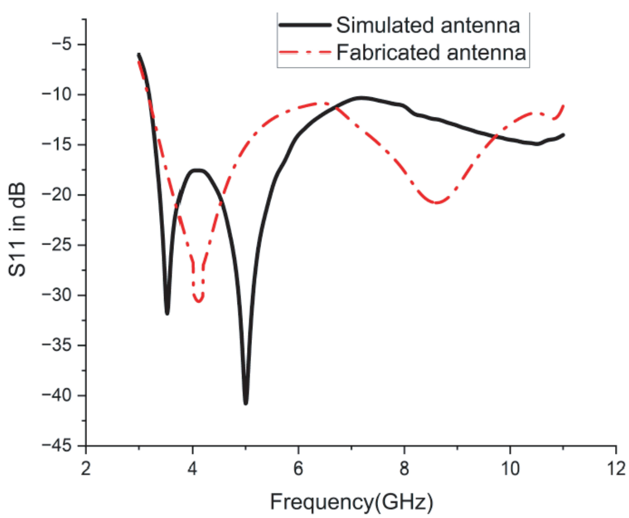

Figure 9. Comparison of measured and simulated results (S_{11}).

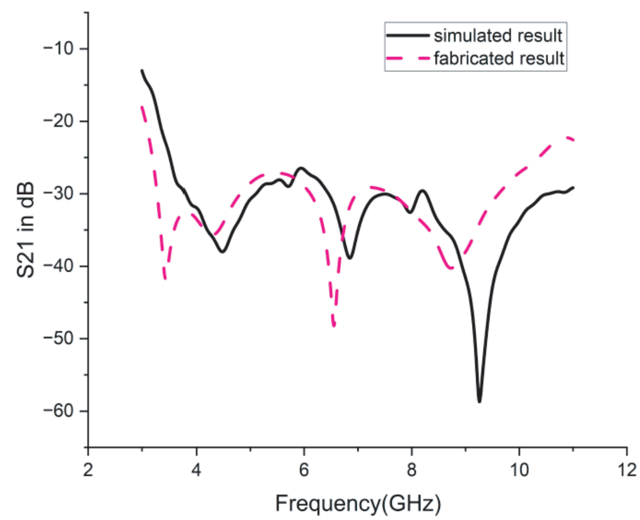

Figure 10. Comparison of measured and simulated results (S_{21}).

3.3. Comparison of Proposed Antenna Performance with Existing Reported Antennas

Based on the above parameters, the fabricated antenna as shown in Figure 8 was tested in an anechoic chamber. Radiation patterns characteristics at different frequencies are shown in Figures 12(a) to 12(d).

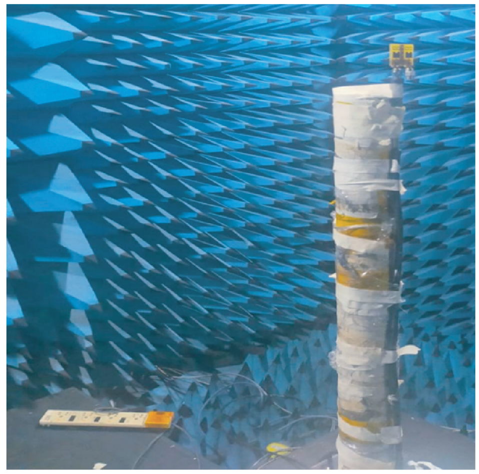

Figure 11. Antenna in anechoic chamber for radiation pattern measurement.

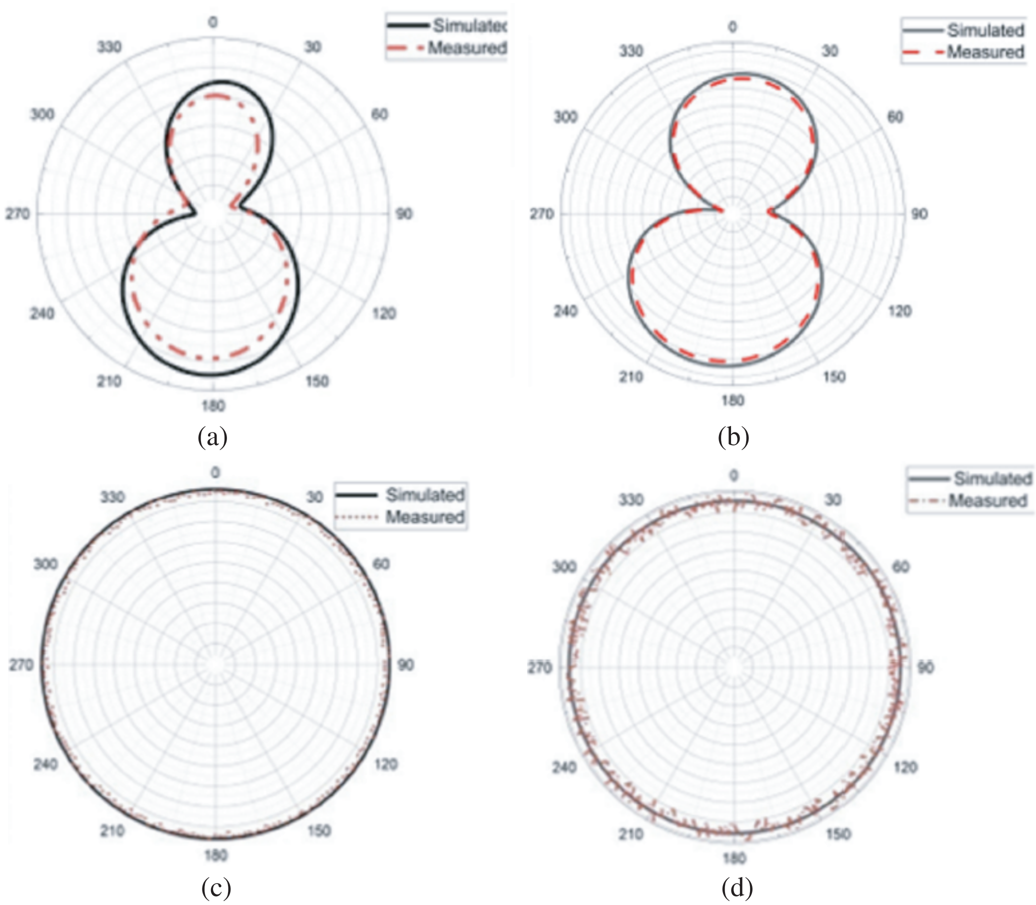

Figure 12. Comparison of radiation pattern, (a) E plane at 5 GHz, (b) E plane at 9.5 GHz, (c) H plane at 5 GHz, (d) H plane at 9.5 GHz.

The measurement setup of an anechoic chamber for measuring radiation patterns is shown in Figure 11, and Figures 12(a) and 12(b) show the simulated and fabricated antenna radiation patterns in E-plane at 5 GHz and 9.5 GHz, respectively. Figures 12(c) and 12(d) show the simulated and fabricated antenna radiation patterns in H-plane at 5 GHz and 9.5 GHz, respectively.

To obtain the radiation pattern experimentally, one port of the antenna is excited (radiating element) whereas the other port is terminated with 50 ohms load. It is observed that there is a decent agreement between the measured and simulated radiation patterns. Small variations in measured and simulated patterns are due to the constraints in reflections from terminated port, connector losses, and experimental setup. It can be noticed from Figure 12 that in the elevation plane, the pattern retains its shape for all frequencies where as in the azimuth plane the pattern shape changes slightly at higher frequencies.

To design the above MIMO antenna by using a defective ground structure, a stub and EBGs with an FR-4 substrate of dielectric constant 4.4, CST studio Suite 2022 are used. The proposed antenna results are also compared with existing reported work and presented in Table 3.

Table 3. Comparison of proposed antenna performance with existing reported antennas.

Literature	Size (mm^2)	Band-width (GHz)	Isolation (dB)	Peak Gain (dB)	ECC	Diversity Gain (dB)
[2]	25×32	3.1–10.6	> 20	–	< 0.05	> 9.99
[6]	50×30	2.5–14.5	> 20	–	< 0.04	> 7.4
[10]	39×39	2.3–13.75	> 22	< 4.6	< 0.02	–
[13]	35×36	3.0–9	> 17	–	< 0.01	> 9.99
[24]	40×40	3.1–10.6	> 20	–	< 0.04	–
[26]	26×26	2.9–11.6	> 16	–	< 0.02	–
[27]	25×25	2.97–13.8	> 15	–	< 0.05	> 9.97
[28]	40×43	3.1–10.6	> 20	< 4	< 0.02	–
[29]	26×31	3.1–11	> 25	< 5.67	< 0.01	> 9.99
[30]	31×26	3.1–11.2	> 20	< 5	< 0.02	–
[31]	39×39	3.1–12.75	> 15	< 5	< 0.02	–
This Work	26×31	3.1–10.6	> 28	< 6.72	< 0.01	> 9.99

4. CONCLUSION

A compact size ($26 \times 31\,\text{mm}^2$) UWB MIMO antenna with EBG structures and low mutual coupling ($S_{21}/S_{12} > -28\,\text{dB}$) within the frequency range of 3.1 GHz–10.6 GHz is proposed. The proposed antenna uses a DGS & stub in the ground plane and a circular slot EBG structure between two rectangular patches. A peak gain of 6.72 dB within UWB was obtained. After fabrication, the designed MIMO antenna was verified for S-parameters and radiation performance. The measured results are found in close agreement with simulated ones, and the antenna has shown very good MIMO diversity performance. A high diversity-gain ($DG > 9.995$) and very low $ECC < 0.01$ make the proposed antenna suitable for MIMO applications in the UWB.

REFERENCES

1. Segovia-Vargas, D., F. J. Herraiz-Martínez, E. Ugarte-Muñooz, L. E. García-Muñoz, and V. González-Posadas, "Quad-frequency linearly-polarized and dual-frequency circularly-polarized microstrip patch antennas with CRLH loading," *Progress In Electromagnetics Research*, Vol. 133, 91–115, 2013.
2. Ul Haq, M. A. and S. Koziel, "Ground plane alterations for design of high-isolation compact wideband MIMO antenna," *IEEE Access*, Vol. 6, 48978–48983, 2018.

3. Alsultan, R. G. S. and G. O. Yetkin, "Mutual coupling reduction of E-shaped MIMO antenna with matrix of C-shaped resonators," *International Journal of Antennas and Propagation*, Vol. 2018, 1–13, 2018.
4. Mohanna, S., A. Farahbakhsh, and S. Tavakoli, "Mutual coupling reduction in two-dimensional array of microstrip antennas using concave rectangular patches," *Journal of Telecommunications*, Vol. 2, No. 2, 64–69, 2010.
5. Wu, G.-C., G.-M. Wang, J.-G. Liang, X.-J. Gao, and L. Zhu, "Novel ultracompact two-dimensional waveguide-based metasurface for electromagnetic coupling reduction 12 Raveendrababu and Pakala of microstrip antenna array," *International Journal of RF and Microwave Computer-Aided Engineering*, Vol. 25, No. 9, 789–794, 2015.
6. Iqbal, A., O. A. Saraereh, A. W. Ahmad, and S. Bashir, "Mutual coupling reduction using F-shaped stubs in UWB-MIMO antenna," *IEEE Access*, Vol. 6, 2755–2759, 2017.
7. Ahmed, M. I., A. Sebak, E. A. Abdallah, and H. Elhennawy, "Mutual coupling reduction using defected ground structure (DGS) for array applications," *2012 15 International Symposium on Antenna Technology and Applied Electromagnetics*, 1–5, IEEE, 2012.
8. Nandigama, S. V., K. Bharath, and R. K. Dasari, "A MIMO PIFA loaded with CSRR-SRR quadruplets for WLAN, ISM Band, and S-/C-band wireless applications," *Progress In Electromagnetics Research B*, Vol. 101, 137–154, 2023.
9. Prabhu, P. and S. Malarvizhi, "Novel double-side EBG based mutual coupling reduction for compact quad port UWB MIMO antenna," *AEU-International Journal of Electronics and Communications*, Vol. 109, 146–156, 2019.
10. Tang, Z., X. Wu, J. Zhan, S. Hu, Z. Xi, and Y. Liu, "Compact UWB-MIMo antenna with high isolation and triple band-notched characteristics," *IEEE Access*, Vol. 7, 19856–19865, 2019.
11. Alsayaghi, A., T. Sabapathy, M. Jusoh, K. Hossain, R. B. Ahmad, M. N. Osman, S. Jayaprakasam, H. A. Rahim, and N. S. Raghava, "Investigation on the mutual coupling reduction in MIMO antenna using dual split CSRR EBG," *Journal of Physics: Conference Series*, Vol. 1962, 012012, IOP Publishing, 2021.
12. Abushamleh, S., H. Al-Rizzo, A. Abbosh, and A. A. Kishk, "Mutual coupling reduction between two patch antennas using a new miniaturized soft surface structure," *2013 IEEE Antennas and Propagation Society International Symposium (APSURSI)*, 1822–1823, IEEE, 2013.
13. Park, J.-D., M. Rahman, and H. N. Chen, "Isolation enhancement of wide-band MIMO array antennas utilizing resistive loading," *IEEE Access*, Vol. 7, 81020–81026, 2019.
14. Farahani, H. S., M. Veysi, M. Kamyab, and A. Tadjalli, "Mutual coupling reduction in patch antenna arrays using a UC-EBG superstrate," *IEEE Antennas and Wireless Propagation Letters*, Vol. 9, 57–59, 2010.
15. Khattak, M. I., M. I. Khan, M. Anab, A. Ullah, M. Al-Hasan, and J. Nebhen, "Miniaturized CPW-fed UWB-MIMO antennas with decoupling stub and enhanced isolation," *International Journal of Microwave and Wireless Technologies*, Vol. 14, No. 4, 456–464, 2022.
16. Fadehan, G. A., Y. O. Olasoji, and K. B. Adedeji, "Mutual coupling effect and reduction method with modified electromagnetic band gap in UWB MIMO antenna," *Applied Sciences*, Vol. 12, No. 23, 12358, 2022.
17. Gollamudi, N. K., Y. V. Narayana, and A. M. Prasad, "Compact and asymmetric fed modified hexagonal shaped multiple-input multiple-output (MIMO) antenna for 5G sub: 6 GHz (n77/n78 & n79) and WLAN applications," *Analog Integrated Circuits and Signal Processing*, Vol. 114, No. 1, 103–112, 2023.
18. Wang, Z., W. Mu, M. Yang, and C. Li, "Design of compact multiband MIMO antenna based on ground neutralization line decoupling," *The Applied Computational Electromagnetics Society Journal (ACES)*, 702–715, 2022.
19. Aghoutane, B., S. Das, M. EL Ghzaoui, B. T. P. Madhav, and H. El Faylali, "A novel dual band high gain 4-port millimeter wave MIMO antenna array for 28/37 GHz 5G applications," *AEU-International Journal of Electronics and Communications*, Vol. 145, 154071, 2022.

20. Khalid, M., S. I. Naqvi, N. Hussain, M. Ur Rahman, Fawad, S. S. Mirjavadi, M. J. Khan, and Y. Amin, "4-port MIMO antenna with defected ground structure for 5G millimeter wave applications," *Electronics*, Vol. 9, No. 1, 71, 2020.
21. Hussain, M., W. A. Awan, E. M. Ali, M. S. Alzaidi, M. Alsharef, D. H. Elkamchouchi, A. Alzahrani, and M. F. A. Sree, "Isolation improvement of parasitic element-loaded dual-band MIMO antenna for mm-Wave applications," *Micromachines*, Vol. 13, No. 11, 1918, 2022.
22. Sghaier, N., A. Belkadi, I. B. Hassine, L. Latrach, and A. Gharsallah, "Millimeter-wave dual-band MIMO antennas for 5G wireless applications," *Journal of Infrared, Millimeter, and Terahertz Waves*, Vol. 44, Nos. 3–4, 297–312, 2023.
23. Roshani, S. and H. Shahveisi, "Mutual coupling reduction in microstrip patch antenna arrays using simple microstrip resonator," *Wireless Personal Communications*, Vol. 126, No. 2, 1665–1677, 2022.
24. Rajkumar, S., A. A. Amala, and K. T. Selvan, "Isolation improvement of UWB MIMO antenna utilising molecule fractal structure," *Electronics Letters*, Vol. 55, No. 10, 576–579, 2019.
25. Valavan, S. E., D. Tran, and A. G. Yarovoy, "Novel dual-band phased array antenna with low mutual coupling characteristics," *The 8th European Conference on Antennas and Propagation (EuCAP 2014)*, 1997–2000, 2014.
26. Li, Z., C. Yin, and X. Zhu, "Compact UWB MIMO vivaldi antenna with dual band-notched characteristics," *IEEE Access*, Vol. 7, 38696–38701, 2019.
27. Singh, H. V. and S. Tripathi, "Compact UWB MIMO antenna with cross-shaped unconnected ground stub using characteristic mode analysis," *Microwave and Optical Technology Letters*, Vol. 61, No. 7, 1874–1881, 2019.
28. Amin, F., R. Saleem, T. Shabbir, S. Ur Rehman, M. Bilal, and M. F. Shafique, "A compact quad-element UWB-MIMO antenna system with parasitic decoupling mechanism," *Applied Sciences*, Vol. 9, No. 11, 2371, 2019.
29. Khan, A., S. Bashir, S. Ghafoor, and K. K. Qureshi, "Mutual coupling reduction using ground stub and EBG in a compact wideband MIMO-antenna," *IEEE Access*, Vol. 9, 40972–40979, 2021.
30. Mchbal, A., N. Amar Touhami, H. Elftouh, and A. Dkiouak, "Mutual coupling reduction using a protruded ground branch structure in a compact UWB OWL-shaped MIMO antenna," *International Journal of Antennas and Propagation*, Vol. 2018, Article ID 4598527, 2018.
31. Patre, S. R. and S. P. Singh, "Shared radiator MIMO antenna for broadband applications," *IET Microwaves, Antennas & Propagation*, Vol. 12, No. 7, 1153–1159, 2018.